Lawrence Berkeley National Laboratory
LBL Publications

Title
Redox chemistry of plutonium and plutonium surrogates in vitrified nuclear wastes

Permalink
https://escholarship.org/uc/item/5wj4b0s0

Journal
Journal of the American Ceramic Society, 105(11)

ISSN
0002-7820

Authors
Darab, John G
Li, Hong
Bucher, Jerome J
et al.

Publication Date
2022-11-01

DOI
10.1111/jace.18632

Peer reviewed

RESEARCH ARTICLE

Journal
American Ceramic Society

Redox chemistry of plutonium and plutonium surrogates in vitrified nuclear wastes

John G. Darab[1] | **Hong Li[1]** | **Jerome J. Bucher[2]** | **Jonathan P. Icenhower[2]** | **Patrick G. Allen[3]** | **David K. Shuh[2]** | **John D. Vienna[1]**

[1]Pacific Northwest National Laboratory, Richland, Washington, USA

[2]Lawrence Berkeley National Laboratory, Berkeley, California, USA

[3]Lawrence Livermore National Laboratory, Livermore, California, USA

Correspondence
John D. Vienna, Pacific Northwest National Laboratory, Richland, WA 99352, USA.
Email: john.vienna@pnnl.gov

Present address
John G. Darab, Bucks County Community College, Department of Science, Technology, Engineering, and Mathematics, Newtown, Pennsylvania, USA
Hong Li, Nippon Electric Glass, Shelby, North Carolina, USA
Jonathan P. Icenhower, Corning Incorporated, Sullivan Park, New York, USA

Abstract

Lanthanide borosilicate glasses containing Pu and the nonradioactive analog element Ce were subjects of an x-ray absorption spectroscopy investigation to quantify the +3/+4 ratio of these redox-sensitive elements. The data show that the dominant oxidation states are +4 for Pu and +3 for Ce. The data also indicate that the reductive potential of glasses can be quantified from a solution chemistry method adapted to glass chemistry, although allowances must be made for glass composition. These data can therefore be used to formulate glass compositions and processing schedules that lead to a controlled oxidation state of Pu in melts. Furthermore, the data show that Ce is a poor analog for Pu behavior in melts and that the suitability of surrogates can be assessed by the evaluation approach presented here. The method demonstrated in this paper can be used to estimate the oxidation states of a range of multi-valent elements as functions of temperature and composition with data from only a single redox couple.

KEYWORDS
borosilicate glass, cerium, LaBS glass, oxidation, plutonium, redox, reduction

1 | INTRODUCTION

The enigma of how to manage plutonium (Pu) that was produced by the world's nuclear powers during the Cold War has not yet been completely solved. According to the current US policy, 61.5 metric tons (t) of Pu that has been declared "excess" to the defense needs will be rendered unattractive for weapons use.[1] No single document describes disposition plans for the entirety of the U.S. surplus Pu inventory. Rather, disposition decisions depend on the form of the Pu, which can lead to different disposition pathways.[1] Several options have been considered for disposition of portions of this excess weapons Pu, including: (1) conversion to UO_2-PuO_2 mixed oxide fuel (MOX) and "burning" in reactors followed by disposal in a deep geologic repository, (2) dilution and disposal in a deep geologic repository, and (3) immobilization in glass or ceramics.[2] The preferred alternative is to burn 34 t of the excess Pu as MOX fuel in commercially available nuclear power reactors (called the MOX Fuel Approach).[3,4] However, the MOX Fuel Fabrication Facility Project was cancelled in October 2018 and National Environmental Policy Act (NEPA) analyses are currently in progress to evaluate alternate disposition paths for the 34 metric tons of Pu previously planned for the MOX Fuel Approach. Additionally, since numerous studies have shown the dilution and disposal option to be technically viable and capable of being executed in a reasonable time frame at a cost consistent with fiscal realities, the US Department of Energy (DOE) has decided to use the dilution and disposal option

for disposition of 13.1 t of Pu.[5,6] Six of the 13.1 t of Pu is in the form of impure wastes, scraps, and process residues while the remaining 7.1 t is comprised of non-pit metal and oxides which had previously been planned for disposition using the MOX Fuel Approach.[4] Additional NEPA analyses will be required to determine the appropriate disposition path for the remainder of excess weapons Pu, which may include immobilization.

The UK currently stores the world's largest stockpile of civilian Pu—projected to reach 140 t.[7] The current UK policy is as follows[8]:

"… for nuclear security reasons the preferred policy for managing the vast majority of UK civil separated plutonium is reuse and it therefore should be converted to MOX fuel for use in civil nuclear reactors. Any remaining plutonium whose condition is such that it cannot be converted into MOX will be immobilized and treated as waste for disposal."

As a result, significant effort is ongoing to develop immobilization technologies for Pu through thermal processes to form glass, ceramics, and glass-ceramics.[9–11]

Many nations in addition to the U.S. and UK have recently studied the immobilization of Pu as a disposition method. Australia, Russia, France, China, and other nations are researching various waste forms, particularly glass, ceramics, and glass-ceramics, for high-actinide wastes.[12–16] The Australian Nuclear Science and Technology Organisation (ANSTO) has worked with the U.S. on weapons Pu immobilization and with the UK on immobilizing impure plutonium residues.[13] Institutions in China have shown interest in actinides, An^{3+} and An^{4+}, immobilization using Nd^{3+} and Ce^{4+} as analogues in pyrochlore[17,18] and zirconolite[19,20] ceramics. One of the studies on zirconolite ceramics was published recently (2020) with UK collaborators, where zirconolite ceramic waste forms were synthesized by microwave sintering.[19] Additionally, iron borophosphate glasses and glass ceramics are also being pursued within China for Pu(III) immobilization.[15] Russia has also been interested in glass, ceramic, and glass ceramic forms for Pu and U immobilization,[14,21,22] including garnet-based ceramics[23] and murataite glass ceramics.[24]

One of the primary methods of stabilizing Pu waste is by vitrification. For example, PuO_2, in the form of fired particulates, can be mixed with glass-forming precursors such as quartz (SiO_2), boric acid (H_3BO_3), K_2CO_3, and Gd_2O_3, or glass frit and melted at temperatures of $\approx 1150°C$ or greater to form a durable waste form. The nature of Pu incorporation (i.e., network former, network modifier, oligomeric species, clusters, etc.) into various glass compositions and how it is affected by melt redox chemistry is still not fully understood. This will have significant effect on loading of Pu.

Glass chemistry plays a vital role in determining the waste loading and oxidation state of Pu. In traditional alkali/alkaline earth borosilicate glasses batched from less than 8 wt% Pu oxide (see for example the PNL 76-100, Karraker Frit, and Eller Frit compositions indicated in Table 1), Pu^{4+} has previously been identified as the predominant redox species using optical measurements.[25,26] X-ray photoelectron spectroscopy (XPS) has been used to characterize the oxidation state of Pu in glass, and it was found that Pu^{4+} was the majority species, with Pu^{3+} accounting for the balance.[27,28] Lopez et al.[29] reported that ~90% of the Pu dissolved in a borosilicate glass at 1200°C was Pu^{4+}, with the balance made up by Pu^{3+}. The studies of Cachia et al.,[30] Lopez et al.,[31] and Deschanels et al.[32] demonstrate that the predominant form of Pu in these glasses is Pu^{4+}; however, Bahl et al.[33] indicated that the solubility of Pu^{4+} is low in typical borosilicate glasses (1.5 wt% PuO_2 at 1200°C melting temperature) but higher solubility can be obtained by increasing the melting temperature, controlling the f_{O_2} during melting, or increasing the basicity of the melt. Stefanovsky et al.[21,22] report that Pu^{4+} in as fabricated glass may slowly oxidize to include small concentrations of Pu^{5+} and Pu^{6+}.

An alternative vitreous waste form is the LaBS or "Loffler" glass,[35] which is composed mainly of Si, B, and rare-earth elements, but devoid of alkalis. In these glasses, target waste loadings can be increased dramatically, with nominal PuO_2 concentrations well over 10 wt%. The lower concentrations or a complete lack of alkali and alkaline earth oxides in these new glass formulations affect the melt basicity, which in turn influences the melt and final glass redox chemistry. Furthermore, these glass formulations contain large concentrations of rare earth element neutron absorbing components such as La_2O_3, Nd_2O_3, and Gd_2O_3, which may govern the structural chemistry and solubility limit of the incorporated Pu. One objective of this study is to evaluate the nominal Pu^{4+}/Pu^{3+} ratio in a typical borosilicate and in a LaBS melt. In conjunction with these data, and from data drawn from the literature, we aim to establish an algorithm by which the oxidation state of Pu can be known as a function of glass composition and processing temperature.

For the transition from laboratory-scale experiments to industrial-scale melter evaluations, researchers could benefit from the availability of a non-radioactive surrogate for Pu that accurately reproduces or predicts its behavior in the melt and in the final waste form. Although no single element can embrace the entire range of chemical and structural behaviors for Pu, it has been suggested that cerium (Ce) may be a promising candidate as a Pu-surrogate for the work discussed herein.[29,30,36–42] A number of investigators have shown that Ce^{4+} is much more easily reduced than Pu^{4+} in traditional alkali

TABLE 1 Glass compositions evaluated in this study

Glass	PNL 76–100	Karraker Frit	Eller Frit	Pu10-IV	Pu11.4-L
Composition in mol% oxide					
Al_2O_3	0	0	0.162	3.11	20.1
B_2O_3	12.7	9.32	7.52	14.7	16.1
CaO	3.32	5.83	5.21	0	0
Cs_2O	0	0	0	0.274	0
Fe_2O_3	0	0	0	2.28	0
Gd_2O_3	0	0	0	2.41	2.26
K_2O	0	0	0.06	1.23	0
La_2O_3	0	0	0	0	3.65
Li_2O	0	8.60	18.3	10.6	0
Na_2O	11.2	19.4	11.9	6.36	0
Nd_2O_3	0	0	0	0	3.65
P_2O_5	0	0	0	1.14	0
PuO_2 or CeO_2	2.00	0.13	0.41	2.85	4.53
SiO_2	61.7	56.7	56.2	55.1	46.3
SrO	0	0	0	0	2.31
TiO_2	3.46	0	0.276	0	0
ZnO	5.68	0	0	0	0
ZrO_2	0	0	0	0	1.01
PuO_2 wt%	8.00	0.600	2.00	10.0	11.4
Basicity value[a]	0.556	0.573	0.574	0.573	0.624
Melt					
Temperature	1250°C	1100°C	1000°C	1300–1500°C	1500°C
Duration	2+ h	4–8 h	12 h	1–3 h	4 h
Atmosphere	Oxygen	Air	Air	Air	Air
Reference	Karim[27]	Karraker[25]	Eller[26]	This work	This work

[a]Basicity calculated using method and coefficients reported by McCloy et al.[34]

boroaluminosilicate glasses;[29–31,43] however, virtually no work has been done to compare the redox chemistry of Ce and Pu in LaBS glass. Thus, another objective of this work is to elucidate the effectiveness of Ce as a surrogate for Pu in LaBS and typical borosilicate glass melts.

2 | CHEMICAL BACKGROUND

Detailed information concerning the chemistry of metal ions, especially actinide ions, in oxide glass systems is unavailable for the complete range of possible processing conditions and/or compositional variables. However, in many cases, the redox and coordination chemistries of metal ions in oxide melts and glasses can be inferred from those in aqueous or complexing systems.[44,45] Thus, a great deal of insight into the chemistry of actinides and their surrogates incorporated into oxide melts and glasses can be gained by first evaluating relevant studies per-

formed in aqueous systems. There are some general trends in the actinides, especially the early members (U, Np, Pu, and Am) that define the chemistry of these elements and assist in the search for a practical non-radioactive surrogate for Pu. We discuss some of these aspects of the relevant actinide chemistry in the subsections below.

2.1 | Redox chemistry of actinides and surrogates

Elemental Pu, the sixth member of the actinide series, has a ground state electronic configuration of $[Rn]5f^67s^2$. In general, Pu has been found to exist in oxidation states ranging from +3 to +7, with those from +3 to +5 being most relevant to glass melts. Many actinide elements are primarily available only in the +3 oxidation state in glass melts, for example, Ac, Am, Cm, Bk, Cf, and Fm. Another common oxidation state is +4, which is shared among

many actinides, including Th, U, and Np, and is the most stable state for Pu (Cotton 1980 pp. 1005–1046[46]; Morss et al. 2006 pp. 974[47]).

2.2 | Structural chemistry of actinides and surrogates

The coordination of +4 actinide species typically exhibits eightfold, dodecahedral or square antiprismatic coordination with oxygen. The actinide dioxides PuO_2, NpO_2, AmO_2, ThO_2, and UO_2 obtain eightfold coordination through crystallization in the fluorite structure. Similarly, eightfold antiprismatic coordination with oxygen occurs in Ce and Hf compounds and crystalline CeO_2 occurs in the fluorite structure (Cotton 1980 pp. 981–1004 and 824–831).[46] Pure HfO_2, however, does not crystallize into the fluorite structure but rather resembles the chemistry of ZrO_2, exhibiting sevenfold coordination with oxygen in the monoclinic (baddeleyite) structure.[46] High temperature or rare-earth or alkaline earth impurities can stabilize HfO_2 or ZrO_2 in the cubic fluorite structure.[48] In addition, new investigations have shown that Hf exists in borosilicate glass as an alkali Hf silicate complex (e.g., $Na_2HfSi_6O_{15}$).[49] Such an alkali Hf silicate complex has a structural arrangement similar to that of the Hf metallasiloxane complex first described by Motevalli et al.[50] However, because of the lack of alkali ions in the LaBS glass studied in this investigation, it is unlikely that a similar Pu complex will form.

In contrast, complexes of actinides in the +3 oxidation state usually exhibit sixfold octahedral coordination with oxygen (Cotton 1980 pp. 1005–1046[46]; Morss et al. 2006, pp. 976[47]). Likewise, the +3 lanthanides in the oxides, Gd_2O_3 for example, have sixfold coordination with oxygen.[51] However, for +3 lanthanide compounds, coordination numbers of 7, 8, or 9 are also common (Cotton 1980 pp. 981–1004).[46]

2.3 | Chemistry in melts and glasses

Consistent with the above observation that the most stable oxidation state for the trans-americium elements in glasses is +3, a single oxidation state (+3) for curium (Cm) and americium (Am) in glass was reported by Assefa[52] and Karraker,[25] respectively. Similarly, consistent with the above observation that in nature Th exists in the +4 oxidation state, Farges[53] and Caulder et al.[49] reported that Th and Hf, respectively, exist in glass in the single oxidation state of +4.

In typical waste glass formulations, Pu is most commonly observed in the +3 and +4 oxidations states.[25–27,30–32,54,55] Bahl et al. have reported the simul-

taneous presence of Pu^{3+}, Pu^{4+}, and a higher oxidation species (likely Pu^{6+}) in a glass melted with Si_3N_4.[33] Surrogates have been used for Pu in glass due to the difficulties obtaining and handling Pu ensuing from the large costs resulting from security, radioactivity, and safety issues. As a result, Ce has often been used as an analog for Pu because both exist in melt in the +3 and +4 oxidation states. However, the oxidation reaction for cerium in melts ($Ce^{3+} + \frac{1}{4}O_2 = Ce^{4+} + \frac{1}{2}O^{2-}$) is significantly more exothermic than the analogous reaction for Pu. Accordingly, Ce^{3+} is more stable at higher melt temperatures compared to Pu^{3+}, and this fact makes comparisons challenging. On the other hand, Hf exists exclusively as a +4 ion yet has a different electron configuration than Pu - $[Xe]4f^{14}5d^26s^2$. Similarly, Gd exists exclusively as a +3 ion. HfO_2 and Gd_2O_3 have been used as surrogates for Pu^{4+} and Pu^{3+}, respectively for solubility studies.[29,56,57] Based on the above discussion, Pu^{4+} might be expected to occur as an eightfold coordinated complex with oxygen in glass melts while, sixfold coordination is expected for Pu^{3+}.

3 | EXPERIMENTAL METHOD

The glasses studied in this work were prepared at Pacific Northwest National Laboratory (PNNL). Glass samples were shipped to Lawrence Berkeley National Laboratory (LBNL), where they and appropriate reference materials were prepared for X-ray absorption spectroscopy (XAS) measurements. The samples were then sent to the Stanford Synchrotron Radiation Lightsource (SSRL), where LBNL and PNNL collaborators conducted the XAS measurements.

Two different sets of Pu- containing glass systems have been investigated in this work: Pu10-IV and Pu11.4-L along with their respective Ce-containing analogs Pu10S-IV and Pu11.4S-L. The nomenclatures used here for the Pu10-IV and Pu11.4-L glasses are different than those that may appear in internal reports or future publications by other authors.[a] Here, the terminology Pu10-IV informs the reader that the glass was developed from a nominal Pu baseline waste glass composition containing 10.0 wt% PuO_2 (Pu10-IV). For the simulated (i.e., non-radioactive) glasses (Pu10S-IV and Pu11.4S-L) containing CeO_2 instead of PuO_2, the molar concentration of CeO_2 was kept identical to that of PuO_2. The base glass series is designated with -IV or with -L.

---

[a] Pu10-IVa and Pu10-IVb have also been referred to as Pu16MC3-2.1#1 and Pu16MC3-2.1#2; Pu11.4-L has been termed V2 by Vienna et al.[58] as well as PuPNL-30-11.4. New nomenclatures have been used to make sample identifications more consistent with those used by Darab et al.[37] and to make this article more readable.

TABLE 2 Nominal and measured composition of Pu11.4-L frit (wt% oxide)

Oxide	Nominal	Measured
Al_2O_3	21.49	21.54
B_2O_3	11.74	11.71
Gd_2O_3	8.59	8.61
La_2O_3	12.43	12.35
Nd_2O_3	12.83	12.80
SrO	2.51	2.51
SiO_2	29.12	29.13
ZrO_2	1.30	1.29
Total	100.00	99.94

TABLE 3 Results of radiochemical analysis on the starting Pu-nitric acid solution

Isotope	Concentration (g/L)
^{238}Pu	0.0000
^{239}Pu	0.1884
^{240}Pu	0.0129
^{241}Pu	0.0004
^{241}Am	0.0000
^{242}Pu	0.0001
Total	0.2018

The Pu10-IV glass is a typical borosilicate glass that is chemically similar to other borosilicate waste glass compositions containing Pu (Table 1). The main differences between Pu10-IV and other glasses are that the former contains four different alkali oxides instead of the typical Na_2O, and that the former contains rare earth oxides. Pu11.4-L is a LaBS glass that is devoid of alkalis, although it contains the alkaline earth SrO. The rare earth element oxides include Gd_2O_3, Nd_2O_3, and La_2O_3.

3.1 | Preparation of frits for plutonium-containing glasses

Two frit compositions were fabricated for melting with Pu or Ce. Batch material was made by mixing appropriate amounts of dry chemical reagents: SiO_2, Al_2O_3, H_3BO_3, $BaCO_3$, Cs_2CO_3, Fe_2O_3, Gd_2O_3, K_2CO_3, La_2O_3, Li_2CO_3, Na_2CO_3, Nd_2O_3, $SrCO_3$, ZrO_2, and Na_2PO_4. Batches of ≈500 g were melted in Pt/10%Rh crucibles in a furnace (Deltech DT-31) at 1250°C for use in the Pu10-IV glass preparation or at 1450°C for use in the Pu11.4-L glass preparation. Melt duration in both cases was 1 h, after which the melt was quenched on a stainless-steel plate and then ground in a tungsten carbide mill for 3 min. Final Pu11.4-L frit composition was confirmed by chemical analysis. Samples were fused in KOH in a Ni crucible and dissolved in HNO_3. The solution was diluted and analyzed using inductively coupled plasma atomic emission spectroscopy (ICP-AES), with results summarized in Table 2.

3.2 | Preparation of low-fired PuO_2 source

The procedure for preparing the low-fired PuO_2 has been described in detail elsewhere.[58] Here we summarize the pertinent information. A 0.35 M nitric acid solution con-

taining the Pu and related isotopes listed in Table 3 was boiled in approximately 0.25 L batches in a Teflon container at a temperature of 200–270°C.[58] After a 10-fold reduction in solution volume was achieved, the liquid was transferred to an alumina crucible and heated in a muffle furnace at a temperature of 270–300°C, forming a dried foamy material that was then calcined between 350°C and 400°C for 30 min for direct denitration/conversion to PuO_2.

3.3 | Preparation of plutonium- and cerium-containing glasses

Frits were mixed with appropriate amounts of PuO_2 source and melted in a Pt-10%Rh crucible in air. Melts were conducted in a radiological glove box. The Pu10-IV glasses were prepared by melting the frit/PuO_2 mixture at 1300°C for 2 h (glass Pu10-IVa), then at 1500°C for 1 h (glass Pu10-IVb). The Pu11.4-L glass was prepared by melting the frit/PuO_2 mixture at 1500°C for 4 h, stirring the melt with an Inconel rod for ~5 s after the first and second hours. Melts were quenched by placing the crucible in a water bath.[b]

Selected samples were examined by powder X-ray diffraction to confirm dissolution of the PuO_2.[58] The composition of glass Pu11.4-L was confirmed using ICP-AES as shown in Table 4.

For the Ce-containing glasses, Pu10S-IVa, Pu10S-IVb, and Pu11.4S-L, CeO_2 was added to the baseline batch material, which was then melted directly (intermediate frits were not prepared). The Ce-containing glasses were prepared in exactly the same manner as their homologous Pu-containing counterparts. The $[Ce^{4+}]/[Ce_{total}]$ ratio in appropriate glass samples was determined using a wet chemical method discussed previously.[41]

---

[b] Slightly different melting procedures were employed because the studies were performed at different times. The impacts are expected to be minimal.

TABLE 4 Nominal and measured composition of Pu11.4-L glass (wt% oxide)

Oxide	Nominal	Measured
Al_2O_3	19.0	22.1
B_2O_3	10.4	10.4
Gd_2O_3	7.60	7.60
La_2O_3	11.0	11.4
Nd_2O_3	11.4	11.7
PuO_2	11.4	9.20
SrO	2.20	2.30
SiO_2	25.8	(a)
ZrO_2	1.20	1.10

(a)SiO_2 concentration was not obtained due to experimental difficulty.

3.4 | XAS measurements

The Ce-containing glasses were ground to -325 mesh ($<44\ \mu m$) in a WC mill and sealed with mylar tape in an aluminum holder. The solid reference materials CeO_2, $Ce_2(SO_4)_3$, and $^{242}PuO_2$ were also prepared in this manner. The Pu-containing glasses, in the form of fractured chips or shards, were sealed in 5 mm-diameter plastic centrifuge tubes by melting the caps directly to the tubes with a soldering iron. Aqueous solutions of 0.020 M Pu^{4+}(aq) or Pu^{3+}(aq) were prepared for measurement as well. The isotope used for the solutions was ^{242}Pu with 0.05 mol% ^{241}Am as the principal transuranic impurity.

All X-ray absorption spectra discussed in this work were obtained at room temperature on beam line 4–1 at SSRL. Cerium or Pu L_{III}-edge X-ray absorption near-edge (XANES) data were obtained in fluorescence mode. References were simultaneously measured in transmission mode. The beam line used a Si (220) double crystal monochromator, standard ionization detectors, and a Ge solid state fluorescence detector developed at LBNL.[59] For each scan, the incident and fluorescence/transmission X-ray intensities were recorded as a function of X-ray energy, E, allowing the absorption coefficient, μ, to be determined.

Data were collected between 5673 eV and 6273 eV for Ce L_{III} XANES or between 18 000 eV and 18 600 eV for Pu L_{III}-edge XAS with the incident beam detuned 50% to decrease the contribution from higher harmonics. Monochromator step increments were 0.2 eV in the vicinity of the Ce L_{III} edge (5693–5733 eV) and 0.5 eV near the Pu L_{III} edge (18 025–18 075 eV). X-ray energies were calibrated using the CeO_2 or PuO_2 reference. Between two and five scans were taken for each sample, depending on the signal to background ratio, and then averaged. For each averaged set of XAFS data, the energy of the main absorption feature was taken as the absorption maximum rather than the half-height of the leading edge from feature for the purposes of this manuscript.
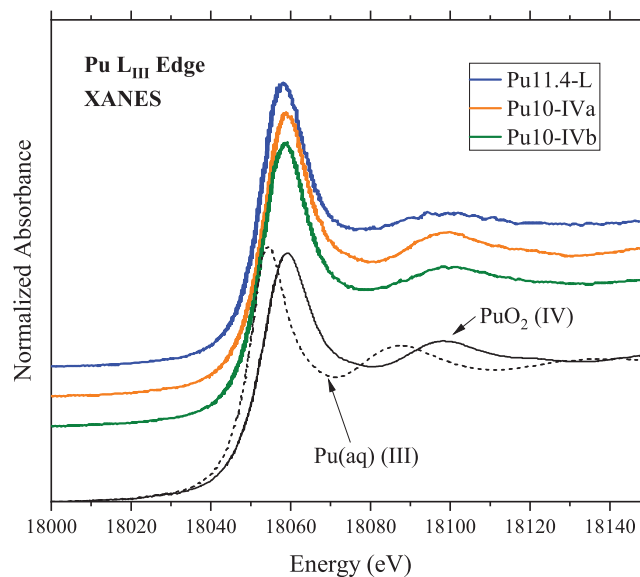

FIGURE 1 X-ray absorption near-edge structure of Pu-L_{III} edge in standards and glasses

4 | RESULTS

4.1 | Redox by chemical method

The $[Ce^{4+}]/[Ce_{total}]$ ratio in the Pu11.4S-L glass was determined to be 0.06 ± 0.01 using a proven wet chemical method.[41] However, this method could not be performed on the Pu10S-IV glasses because these compositions contained considerable concentrations of Fe_2O_3, which interfered with the analysis.

4.2 | X-ray absorption measurements

Figure 1 shows a detail of the Pu L_{III}-edge XANES spectra obtained from the Pu-containing glasses along with those obtained from the PuO_2(s) and Pu^{3+}(aq) reference materials. Note that the main peak position of the Pu in the glasses lines up closely with, but is slightly lower in energy than, that for the PuO_2(s) reference and the Pu^{4+}(aq) reference (not shown). This indicates that Pu^{4+} is the predominant species in these glasses, but that a small contribution from Pu^{3+} (the main absorption peak, which occurs at a significantly lower energy than that for Pu^{4+}, see below) also exists.

Figure 2 shows a detail of the Ce L_{III}-edge XANES region obtained from the Ce-containing glasses along with those obtained from the CeO_2 and $Ce_2(SO_4)_3$ reference materials. Note that the main peak position of the cerium in the glasses lines up closely to that of the $Ce_2(SO_4)_3$ reference, indicating that Ce^{3+} is the predominant species in these glasses. Antonio et al. found a sharp Ce^{3+} edge at 5723 eV in
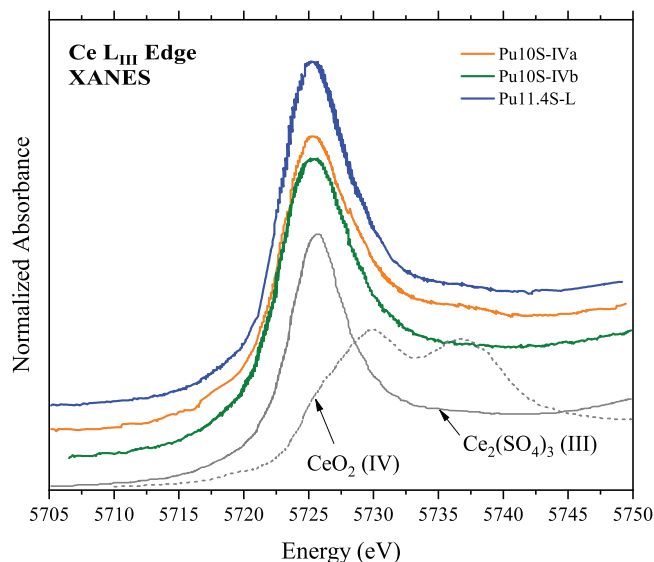
FIGURE 2 X-ray absorption near-edge structure of Ce-L_{III} edge in standards and glasses

Ce_2MoO_6, consistent with the results for $Ce_2(SO_4)_3$.[60] Furthermore, the XANES peak observed at approximately 5740 eV for the CeO_2 reference is characteristic of Ce^{4+} species in general,[37,61–63] and as such can be used as a Ce^{4+} signature. The lack of any XANES feature near 5740 eV for the Pu11.4S-L glass indicates that an insignificant amount of Ce^{4+} is present. Some intensity is observed near 5740 eV for the Pu10S-IV glasses, however, indicating that a small contribution from Ce^{4+} is present in these samples.

5 | DISCUSSION

5.1 | Analysis of XAFS data

For a given element in a compound or material, the energy at which the main absorption edge occurs is sensitive to oxidation state.[64] For a compound or material with mixed metal oxidation states, the XAFS spectrum obtained can typically be approximated as a mixture of contributions from the X-ray absorptions from each of the individual metal oxidation states/environments. In many cases, the contributing XAFS features are not well-resolved, and the measured overall spectrum is a summation of the features from the individual species. Thus, the peak position, $E_{peak}^{Pu-meas}$, for a sample can be approximated using a typical rule-of-mixtures approach:

$$E_{peak}^{Pu-meas} = E_{peak}^{Pu^{4+}} x_{Pu^{4+}} + E_{peak}^{Pu^{3+}} x_{Pu^{3+}} \quad (1)$$

where $E_{peak}^{Pu^{4+}}$ and $E_{peak}^{Pu^{3+}}$ are the peak positions for pure Pu^{4+} and Pu^{3+} reference compounds, and $x_{Pu^{4+}}$ and $x_{Pu^{3+}}$ are the fractions of Pu^{4+} and Pu^{3+} in the glass with the sum of

$x_{Pu^{4+}}$ and $x_{Pu^{3+}}$ equal to unity. A similar expression can be written for the overall Ce peak position.

Here, we have used solid CeO_2, $Ce_2(SO_4)_3$, and PuO_2 as well as $Pu^{4+}(aq)$ as references for Ce^{4+}, Ce^{3+}, and Pu^{4+}. Since there were no readily available pure Pu^{3+} solid reference materials, an aqueous solution containing Pu^{3+} was used instead. The measured peak positions, E_0, obtained from these reference compounds (with known single oxidation state), which are summarized in Table 5, allowed us to define the values of $E_0(Pu^{4+})$, $E_0(Pu^{3+})$, $E_0(Ce^{4+})$, and $E_0(Ce^{3+})$. The peak positions for the Pu- and Ce-containing glasses studied here are also summarized in Table 5, as are the percentages of M^{3+} and M^{4+} determined from Equation (1).

The results summarized in Table 5 indicate that for the glass compositions and melt conditions employed here, Pu occurs predominantly (greater than ≈75%) as Pu^{4+} whereas Ce^{3+} is the principal oxidation state for cerium (greater than ≈95%). The Ce XANES results obtained for the Pu11.4S-L glass (i.e., >95% of the cerium occurs as Ce^{3+}) are corroborated by the results obtained from the chemical analysis of the same glass (i.e., 94% of the cerium occurs as Ce^{3+}). These results suggest that Ce is not a good surrogate for Pu for these glasses, due to the differences in oxidation state. However, the influence of using a Ce^{3+} surrogate for Pu^{3+} or a Ce^{4+} surrogate for Pu^{4+} on glass properties was not evaluated due to the challenge in producing glasses with purely Pu^{3+} and Ce^{4+}, respectively.

5.2 | Glass redox chemistry

From the analyses discussed above, where it is apparent that Ce is an inappropriate surrogate for Pu for the glass compositions and processing conditions explored, it would be useful to obtain a more thorough understanding of the redox chemistry of Ce and Pu in glasses of differing composition and/or processing conditions that may define a set of conditions where Ce is a good surrogate for Pu, e.g., where Ce^{4+} is stable and dominant in the melt like Pu^{4+} under relative oxidizing conditions.

The redox chemistry of various metal species in glass-forming oxide melts has previously been investigated at various temperatures, primarily by Schreiber and co-workers,[44,65,66] although information concerning the redox chemistry of Pu in such melts was not available. The details concerning Schreiber's work and subsequent analyses by this team are presented in Supporting Information. One of the rudimentary expressions from these analyses is presented here:

$$\log \frac{[M^{(n-1)+}]}{[M^{n+}]} = \varepsilon_M \text{ (melt)} - 0.25 \log[f_{O_2}] \quad (2)$$

TABLE 5 X-ray edge energies (given as white line feature maximum) measured in glasses and standards with estimated redox couple concentrations

Sample	Edge	E_0 (eV)	Reference value	M^{3+} (%)	M^{4+} (%)
PuO_2	Pu L_{III}	18 059.2	E_0 (Pu^{4+})	0	100
Pu^{3+} (aq)	Pu L_{III}	18 054.5	E_0 (Pu^{3+})	100	0
Pu10-IVa	Pu L_{III}	18 058.9		6 ± 5	94 ± 5
Pu10-IVb	Pu L_{III}	18 058.6		13 ± 5	87 ± 5
Pu11.4-L	Pu L_{III}	18 058.1		23 ± 5	77 ± 5
CeO_2	Ce L_{III}	5729.9	E_0 (Ce^{4+})	0	100
$Ce_2(SO_4)_3$	Ce L_{III}	5725.6	E_0 (Ce^{3+})	100	0
Pu10S-IVa	Ce L_{III}	5725.3		>95	<5
Pu10S-IVb	Ce L_{III}	5725.2		>95	<5
Pu11.4S-L	Ce L_{III}	5725.1		>95	<5

TABLE 6 ε_M (melt) values for Pu and Ce in LaBS glasses

Sample	M	$[M^{3+}]/[M^{4+}]$	ε_M (melt) Mean	ε_M (melt) Range
Pu10-IVa	Pu	0.064 ± 0.057	−1.4	−2.3 to −1.1
Pu10-IVb	Pu	0.15 ± 0.06	−1.0	−1.2 to −0.85
Pu11.4-L	Pu	0.30 ± 0.08	−0.70	−0.84 to −0.60
Pu11.4S-L	Ce	16 ± 3	+1.0	+0.9 to +1.1

where $[M^{(n-1)+}]/[M^{n+}]$ is the ratio of reduced to oxidized species in a melt, ε_M(melt) is the relative reduction potential of the metal M in the melt, and f_{O_2} is the corresponding oxygen fugacity. Others have also measured actinide redox properties in individual borosilicate or silicate glasses (examples given in Refs.[25–27,30,31,33,67]) but not in Pu11.4-L LaBS glass, nor as functions of glass composition.

For the Ce-containing Pu11.4S-L quenched glass studied here, only Ce^{3+} was detected by XANES, that is, $[Ce^{4+}]/[Ce_{total}]$ is less than ≈0.05 (the XAFS detection limit for Ce^{4+}). The chemical analysis performed on this same glass allows us to get a more definitive assessment of the redox chemistry of Ce in the Pu11.4S-L glass and indicated that $[Ce^{4+}]/[Ce_{total}]$ was 0.06 (±0.01). A reasonable value of $[Ce^{4+}]/[Ce_{total}]$ for this glass would thus be 0.06 ± 0.01. We also determined the value of $[Pu^{4+}]/[Pu_{total}]$ for the glasses studied here directly from the XAFS results. As previously mentioned, chemical analyses could not be performed on the Pu10S-IV glasses, so there is no more definitive $[Ce^{4+}]/[Ce_{total}]$ value for these glasses.

The $[M^{4+}]/[M_{total}]$ values determined above were then converted to $[M^{3+}]/[M^{4+}]$ values (see Table 6). Assuming that the value of $[M^{3+}]/[M^{4+}]$ in the quenched glasses is representative of those in the corresponding melts at melt temperature,[c] the value of ε_M(melt) of the appropriate couple in the melt can be calculated from Equation (2). The calculated values of ε_M(melt) for the particular glass compositions and melt conditions employed here are summarized in Table 6. As in the previous section, the large difference between the mean value of ε_{Ce}(Pu11.4S-L) of +1.0 for Ce in the Pu11.4S-L glass and the mean value of ε_{Pu}(Pu11.4-L) of −0.7 for Pu in the Pu11.4-L glass substantiates a large difference between the redox chemistry of Ce and Pu in these glasses.

5.3 | Melt redox chemistry

While we have established in the preceding two sections that the redox chemistry of Ce and Pu are dramatically different for the glasses studied here, it would be beneficial to verify these results using an alternative based on melt chemistry.

The extensive work of Schreiber et al.,[44,65,66] and in particular the Savannah River Laboratory-131 (SRL-131) glass and melt composition,[65] provides this opportunity, although as mentioned previously Pu is not included in these studies. A correlation in redox couples between melts of different compositions and processing temperatures, ε_M(melt), with respect to that of SRL-131 melts at 1150°C, ε_M(SRL), was identified based on the work of Schreiber (See the Supporting Information for details).[65] This relation is:

$$\varepsilon_M(melt) = b \times \varepsilon_M(SRL) + \delta \ [\pm 0.4 \text{units}] \quad (3)$$

---

[c] A reasonable assumption due to the rapid quenching of glasses relative to the kinetics of oxygen transport in the melt.

TABLE 7 Comparison of standard aqueous redox potentials with those in SRL-131 and Pu11.4-L glass melts

	I	II	III
Solvent	Water	SRL-131	Pu11.4-L
Value	ε^0_M	$\varepsilon_M(SRL)^{a)}$	$\varepsilon_M(Pu11.4\text{-}L)^{a)}$
Couple			
$Ce^{4+/3+}$	$+1.44$ $V^{b)}$	$+0.2^{c)}$ $-0.1^{d)}$	$+1.0^{e)}$
$Pu^{4+/3+}$	$+0.97$ $V^{f)}$	$-1.5^{c)}$	$-0.4^{g)}$ $-0.7^{h)}$

a) ε_M is a unitless value.

b) Versus SHE from Schreiber.[44]

c) Value determined by extrapolating from the aqueous reduction potential listed in column I using Equation (4).

d) Experimentally measured value.[44]

e) Mean value determined from Ce chemical/XANES data.

f) Versus NHE from Nugent.[68]

g) Value determined by extrapolating from the $Pu^{4+/3+}$ SRL-131 reduction potential predicted from the measured $Ce^{4+/3+}$ potential listed in column II using Equation (5). Combined standard deviation is approximately ± 0.4 units.

h) Mean value determined from Pu XANES data.

where b is equal to T_{SRL}/T_{melt} (the ratio of the absolute melt temperature of the SRL-131 system to that of the melt system in question) and δ is related to b and the ratio of activity coefficients for the metal redox ions in a given melt, the oxygen fugacity (f_{O_2}) in the melt, and the number of electrons transferred in the redox couple. More details on derivation of Equation (3) are reported in Supporting Information.

To obtain the alternative analyses of the melt redox chemistry of Ce and Pu desired in this study, Equation (3) needs to be evaluated. To do that, we need to (among other things) determine the value of $\varepsilon_{Pu}(SRL)$, which is not part of Schreiber's data set.

To accomplish this, we have relied on Schreiber and co-workers,[44,65,66] who demonstrated the useful comparability of the electromotive force series in silicate-based melts to those from aqueous solutions. For example, in redox reactions involving one electron, the standard reduction potential of 12 couples in aqueous solution, $\varepsilon^0_M(aq)(V, SHE)$, and the unitless relative (reference) reduction potential in alkali borosilicate SRL-131 melts at 1150°C, $\varepsilon_M(SRL)$,[44] can be correlated ($R^2 = 0.97$) using the following expression:

$$\varepsilon_M(SRL) = -5.1 + 3.7(V^{-1})\varepsilon^0_M(aq) \ [\pm 0.4 \text{ units}] \quad (4)$$

The aqueous redox potentials for the $Ce^{4+/3+}$ and $Pu^{4+/3+}$ couples are listed in column I of Table 7.[44,68] Using Equation (4), the reduction potentials for these couples in the SRL-131 melt were evaluated and are summarized in column II of Table 7. For the Pu11.4-L (and Pu11.4S-L) melts at 1500°C melt temperature, the value of b needed for
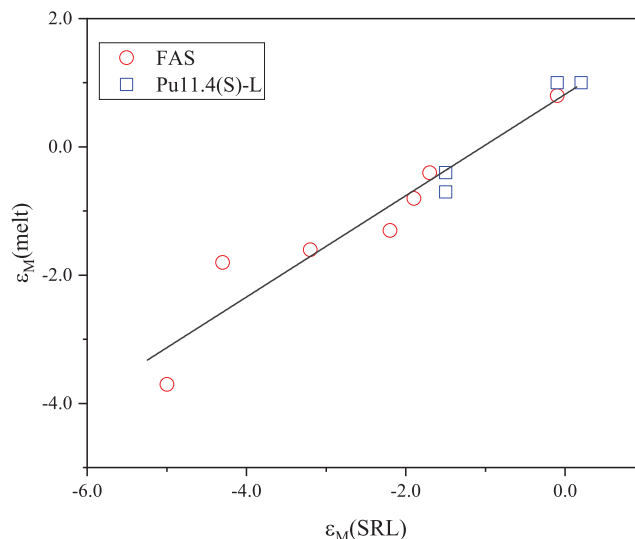
FIGURE 3 Comparison of ε_M values between Pu11.4-L, FAS, and SRL glasses

Equation (3) was calculated to be 0.80 based on the relative melt temperatures. For the Pu11.4S-L melt, where the value of $\varepsilon_{Ce}(Pu11.4S\text{-}L)$ was estimated to be 1.0 (Table 6), using the calculated value of $\varepsilon_{Ce}(SRL)$ (Table 7), Equation (3) allows us to estimate the value of δ for the Pu11.4-L (and Pu11.4S-L) melts at 1500°C to be 0.8. Thus, for the Pu11.4-L melts at 1500°C in general,

$$\varepsilon_M(Pu11.4\text{-}L) = 0.80\varepsilon_M(SRL) + 0.8 \quad (5)$$

Using the calculated value of $\varepsilon_{Pu}(SRL)$ (Table 7) and Equation (5), the value of $\varepsilon_{Pu}(Pu11.4\text{-}L)$ was determined to be -0.4 (see Table 7). This result is within the experimental error of the measured range, which was determined from the Pu XANES data.

5.4 | Applicability of approach

The approach outlined and validated herein has clear applicability to a variety of related glass research areas. One example might include research in developing new glasses to influence the redox chemistry of species that are not commonly assessable due to safety reasons, such as Pu. In such a case, one could study the redox chemistry of other species, such as Fe, using a variety of techniques to assess the $[M^{(n-1)+}]/[M^{n+}]$ ratio and, in a similar fashion as exemplified herein, estimate the redox chemistry of species of interest in the same glass.

Another example would be using the redox chemistry of a species as a probe to assess the chemistry of the glass matrix ("solvent") itself. Figure 3 shows a plot of $\varepsilon_M(melt)$ versus $\varepsilon_M(SRL)$ for data obtained from both the

Pu11.4-L glass system studied here (Table 6) and those of the FAS (forsterite-anorthite-silica) glass system also studied by Schreiber.[65] Both glass systems used the same melt temperature. Notice that the data fall on the same line. Analyses using Equation (3) allows one to determine that this coincidence of data means that the activity coefficients of species in these melts (through δ) are similar, which may mean the chemical behavior of these melts as a solvent is similar.

Lastly, one can use this approach to identify surrogates for Pu that would better match the desired redox properties than Ce. Consider two different sets of ionic metal species, M_a and M_b, in otherwise identical glass compositions melted under identical conditions. Using Equation (2), we can define the following:

$$\log \frac{\left[M_a^{(n-1)+}\right]}{\left[M_a^{n+}\right]} = \varepsilon_{M_a} - 0.25 \log[f_{O_2}] \quad (6)$$

$$\log \frac{\left[M_b^{(n-1)+}\right]}{\left[M_b^{n+}\right]} = \varepsilon_{M_b} - 0.25 \log[f_{O_2}] \quad (7)$$

Subtracting Equation (6) from Equation (7) and rearranging,

$$\log \frac{\left[M_a^{(n-1)+}\right]}{\left[M_a^{n+}\right]} = \log \frac{\left[M_b^{(n-1)+}\right]}{\left[M_b^{n+}\right]} + \varepsilon_{M_a} - \varepsilon_{M_b} \quad (8)$$

Comparing the Ce^{3+}:Ce^{4+} and Pu^{3+}:Pu^{4+} couples,

$$\log \frac{\left[Ce^{3+}\right]}{\left[Ce^{4+}\right]} = \log \frac{\left[Pu^{3+}\right]}{\left[Pu^{4+}\right]} + 1.7 \quad (9)$$

or more generally for a Pu-surrogate, M_a,

$$\log \frac{\left[M_a^{3+}\right]}{\left[M_a^{4+}\right]} = \log \frac{\left[Pu^{3+}\right]}{\left[Pu^{4+}\right]} + \varepsilon_{M_a} + 0.7 \quad (10)$$

Figure 4 demonstrates the utility of this relationship in estimating the ratios of various redox couples as a function of the $Pu^{4+}/(Pu^{3+} + Pu^{4+})$. In this case the constant 0.7 is specific to this glass composition. Similar relationships were calculated for $Cr^{3+}/(Cr^{3+} + Cr^{6+})$ by Hrma.[69,70] Figure 4 further confirms that Ce is not a good surrogate for Pu, at least in terms of redox chemistry in glass melts, for example between 0.0 and 0.5 $Pu^{4+}/(Pu^{4+}+Pu^{3+})$. Note that the chemical behavior of Fe has served as an analog and inspiration for the development of a class of the most stable chelators for Pu.[71] Although Fe might not be a good surrogate for Pu for structural or solubility studies, once
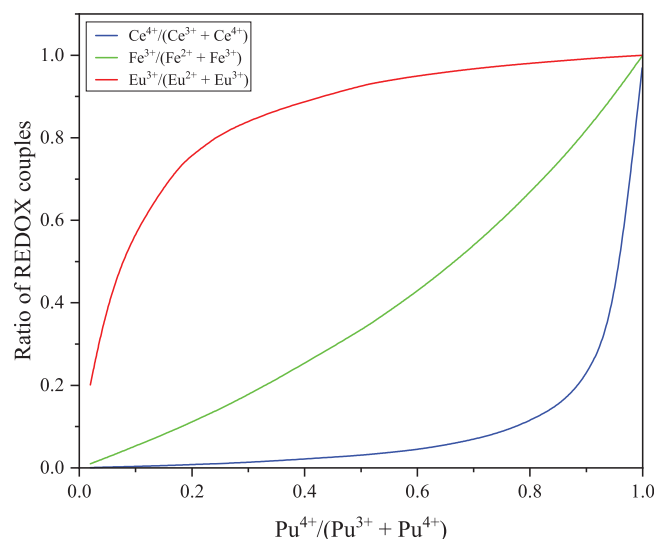

FIGURE 4 Ratio of selected redox couples in glass melts as a function of $Pu^{4+}/(Pu^{3+} + Pu^{4+})$

an estimate of the relative amounts of Pu^{4+} and Pu^{3+} is determined through a correlation with the determined Fe redox chemistry, the appropriate ratios of HfO_2 and Gd_2O_3, as mentioned above, can then be used to estimate the solubilities of Pu^{4+} and Pu^{3+}, respectively. For those melts that are sufficiently oxidizing so that Pu is predominantly in the +4 oxidation state, HfO_2 alone might be a good surrogate for PuO_2, although the coordination environment might be slightly different.[49]

6 | CONCLUSIONS

Using XANES, we have demonstrated that for alkali borosilicate glasses batched with 10 wt% PuO_2 or equimolar CeO_2 and melted at 1300–1500°C in air, Ce is an inappropriate surrogate for Pu. A similar conclusion was achieved using XANES and chemical analyses for LaBS "Loffler" glasses batched with 11.4 wt% PuO_2 or equimolar CeO_2 and melted at 1500°C in air. For both glass systems, the Ce occurs predominantly (~95%) as Ce^{3+} whereas the Pu occurs as >77% Pu^{4+} with the remaining balance as Pu^{3+}. Further analyses of the melt redox chemistries of Ce and Pu in LaBS glass and comparisons with those from aqueous and SRL-131 glass-forming systems support the XANES and chemical results. Based on these combined results for the glasses studied here and for other glass-forming systems that may be more reducing, Ce would not be a good redox surrogate for Pu since the measured $[Ce^{4+}]/[Ce_{total}]$ ratio would remain relatively invariant at <0.05 for similar or more highly reducing melts, whereas the $[Pu^{4+}]/[Pu_{total}]$ ratio would vary significantly under the same conditions. Therefore, we conclude that Ce is a

poor analog for determining the behavior of Pu in alkali borosilicate and LaBS glass compositions. For LaBS glasses and glasses with higher oxidation potentials, Hf oxidation state is more similar to that of Pu, but with a different coordination environment (7) unless stabilized in the cubic structure by rare-earth or alkaline-earth additions. These analyses confirm that there is not a good single non-radioactive surrogate for Pu in glass melts. There is a reason that Pu resides in its own box on the periodic table.

ORCID

Hong Li https://orcid.org/0000-0001-6289-727X
John D. Vienna https://orcid.org/0000-0002-6832-9502

REFERENCES

1. NAS. Review of the Department of Energy's plans for disposal of surplus plutonium in the waste isolation pilot plant. Washington, DC: National Academies of Sciences, Engineering, and Medicine; 2020.
2. DOE. Record of decision for the storage and disposition of weapons-usable fissile materials final programmatic environmental impact statement, FR62:13. Washington, DC: U.S. Department of Energy, Federal Register; 1997.
3. DOE. Surplus plutonium disposition final environmental impact statement, DOE/EIS-0283. Washington, DC: U.S. Department of Energy, Office of Fissile Materials Disposition; 1999.
4. DOE. Surplus plutonium disposition: amended record of decision, 68FR20134. Washington, DC: U.S. Department of Energy, Federal Register; 2003.
5. DOE. Surplus plutonium disposition: record of decision, FR81:65. Washington, DC: U.S. Department of Energy, Federal Register; 2016.
6. DOE. Surplus plutonium disposition: record of decision, 85FR53350. Washington, DC: U.S. Department of Energy, Federal Register; 2020.
7. Hyatt NC. Plutonium management policy in the United Kingdom: the need for a dual track strategy. Energy Policy. 2017;101:303–309.
8. UK D. Management of the UK's plutonium stocks: consultation response on the long-term management of UK-owned separated civil plutonium. London: UK Department of Energy and Climate Change; 2011.
9. Blackburn LR, Sun SK, Lawson SM, Gardner LJ, Ding H, Corkhill CL, et al. Synthesis and characterisation of $Ca_{1-x}Ce_xZrTi_{2-2x}Cr_{2x}O_7$: analogue zirconolite wasteform for the immobilisation of stockpiled UK plutonium. J Eur Ceram Soc. 2020;40:5909–5919. https://doi.org/10.1016/j.jeurceramsoc.2020.05.066
10. Hyatt NC. Plutonium management policy in the United Kingdom: the need for a dual track strategy. Energy Policy. 2017;101:303–309. https://doi.org/10.1016/j.enpol.2016.08.033
11. Thornber SM, Heath PG, Da Costa GP, Stennett MC, Hyatt NC. The effect of pre-treatment parameters on the quality of glass-ceramic wasteforms for plutonium immobilisation, consolidated by hot isostatic pressing. J Nucl Mater. 2017;485:253–261. https://doi.org/10.1016/j.jnucmat.2016.12.028
12. Bhuiyan A, Wong V, Abraham JL, Aughterson RD, Kong L, Farzana R, et al. Phase assemblage and microstructures of $Gd_2Ti_{2-x}Zr_xO_7$ (X = 0.1–0.3) pyrochlore glass-ceramics as potential waste forms for actinide immobilization. Mater Chem Phys. 2021;273:125058. https://doi.org/10.1016/j.matchemphys.2021.125058
13. Gregg DJ, Vance ER. Synroc tailored waste forms for actinide immobilization. Radiochim Acta. 2017;105(11):907–925. https://doi.org/10.1515/ract-2016-2604
14. Stefanovsky SV, Yudintsev SV, Vinokurov SE, Myasoedov BF. Chemical-technological and mineralogical-geochemical aspects of the radioactive waste management. Geochem Int. 2016;54:1136–1155. https://doi.org/10.1134/S001670291613019X
15. Wang F, Liao Q, Dai Y, Zhu HM. Immobilization of gadolinium in iron borophosphate glasses and iron borophosphate based glass-ceramics: implications for the immobilization of plutonium(III). J Nucl Mater. 2016;477:50–58. https://doi.org/10.1016/j.jnucmat.2016.05.006
16. Zhang Y, Gregg DJ, Kong L, Jovanovich M, Triani G. Zirconolite glass-ceramics for plutonium immobilization: the effects of processing redox conditions on charge compensation and durability. J Nucl Mater. 2017;490:238–241. https://doi.org/10.1016/j.jnucmat.2017.04.015
17. Luo F, Tang H, Shu X, Chen Z, Xu C, Wei G, et al. Immobilization of simulated An^{3+} into synthetic $Gd_2Zr_2O_7$ ceramic by SPS without occupation or valence design. Ceram Int. 2021;47:6329–6335. https://doi.org/10.1016/j.ceramint.2020.10.211
18. Wang L, Shu X, Yi F, Shao D, Zhang K, Zhang H, et al. Rapid fabrication and phase transition of Nd and Ce Co-doped $Gd_2Zr_2O_7$

ceramics by SPS. J Eur Ceram Soc. 2018;38:2863–2870. https://doi.org/10.1016/j.jeurceramsoc.2018.02.024

19. Wei ZJ, Blackburn LR, Gardner LJ, Tan SH, Sun SK, Guo WM, et al. Rapid synthesis of zirconolite ceramic wasteform by microwave sintering for disposition of plutonium. J Nucl Mater. 2020;539:152332. https://doi.org/10.1016/j.jnucmat.2020.152332

20. Zhang K, Yin D, Xu K, Zhang H. Self-propagating synthesis and characterization studies of Gd-bearing Hf-zirconolite ceramic waste forms. Materials. 2019;12(1):178. https://doi.org/10.3390/ma12010178

21. Stefanovsky SV, Ptashkin AG, Shiryaev AA, Zubavitchus JV, Veligjanin AA, Marra JC, Chukalina MV. XAFS of Pu L(III) edge in LABS glass. Ceram Trans. 2010;217:17–24.

22. Stefanovsky SV, Shiryaev AA, Zubavichus YV, Marra JC. Plutonium environment in lanthanide borosilicate glass. MRS Online Proc Library. 2010;1264:1109.

23. Alekseeva LS, Nokhrin AV, Boldin MS, Lantsev EA, Orlova AI, Chuvil'deev VN. Hydrolytic stability of $Y_{2.5}Nd_{0.5}Al_5O_{12}$-based garnet ceramics under hydrothermal conditions. Inorg Mater. 2021;57:874–877. https://doi.org/10.1134/S002016852108001X

24. Poglyad SS, Pryzhevskaya EA, Lizin AA, Tomilin SV, Murasova OV. On possibility of the murataite fusion temperature lowering for radioactive waste immobilisation. J Phys Conf Ser. 2018;1133:012019. https://doi.org/10.1088/1742-6596/1133/1/012019

25. Karraker DG. Actinide valences in borosilicate glass. J Am Ceram Soc. 1982;65:53–55.

26. Eller PG, Jarvinen GD, Purson JD, Penneman RA, Ryan RR, Lytle FW, et al. Actinide valances in borosilicate glasses. Radiochim Acta. 1985;39(1):17–22. https://doi.org/10.1524/ract.1985.39.1.17

27. Karim DP, Lam DJ, Diamond H, Friedman AM, Coles DG, Bazan F, et al. XPS valence state determination of Np and Pu in multicomponent borosilicate glass and application to leached 76-68 waste glass surfaces. Scientific Basis for Nuclear Waste Management. MRS Online Proc Library. 1982;6(1):67–73.

28. Maslakov KI, Stefanovsky SV, Teterin AY, Teterin YA, Marra JC. X-ray photoelectron study of lanthanide borosilicate glass. Glass Phys Chem. 2009;35(1):21–27. https://doi.org/10.1134/S1087659609010039

29. Lopez C, Deschanels X, Bart JM, Boubals JM, Den Auwer C, Simoni E. Solubility of actinide surrogates in nuclear glasses. J Nucl Mater. 2003;312:76–80.

30. Cachia JN, Deschanels X, Den Auwer C, Pinet O, Phalippou J, Hennig C, et al. Enhancing cerium and plutonium solubility by reduction in borosilicate glass. J Nucl Mater. 2006;352(1–3):182–189. https://doi.org/10.1016/j.jnucmat.2006.02.052

31. Lopez C, Deschanels X, Den Auwer C, Cachia JN, Peuget S, Bart JM. X-ray absorption studies of borosilicate glasses containing dissolved actinides or surrogates. Phys Scr. 2005;T115:342–345.

32. Deschanels X, Peuget S, Cachia JN, Charpentier T. Plutonium solubility and self-irradiation effects in borosilicate glass. Prog Nucl Energy. 2007;49(8):623–634. https://doi.org/10.1016/j.pnucene.2007.05.001

33. Bahl S, Peuget S, Pidchenko I, Pruessmann T, Rothe J, Dardenne K, et al. Pu coexists in three oxidation states in a borosilicate glass: implications for Pu solubility. Inorg Chem. 2017;56(22):13982–13990. https://doi.org/10.1021/acs.inorgchem.7b02118

34. McCloy JS, Schweiger MJ, Rodriguez CP, Vienna JD. Nepheline crystallization in nuclear waste glasses: progress toward acceptance of high-alumina formulations. Int J Appl Glass Sci. 2011;2(3):201–214. https://doi.org/10.1111/j.2041-1294.2011.00055.x

35. Ramsey WG, Bibler NE, Meaker TF. Compositions and durabilities of glasses for immobilization of plutonium and uranium. Waste Management Symp. 1995;38-4. Available from: https://www.osti.gov/servlets/purl/63953

36. Dacheux N, Clavier N, Ribisson AC, Terra O, Audubert F, Lartigue JE, et al. Immobilisation of actinides in phosphate matrices. C. R. Chimie. 2004;7:1141–1152.

37. Darab JG, Li H, Vienna JD. X-ray absorption spectroscopic investigation of the environment of cerium in glasses based on complex cerium alkali borosilicate compositions. J Non-Cryst Solids. 1998;226(1–2):162–174. Available from: https://doi.org/10.1016/S0022-3093(98)00369-X

38. Bulkley SA, Vienna JD. Composition effects on viscosity and chemical durability of simulated plutonium residue glasses. Scientific basis for nuclear waste management XX. Materials Research Society 1997;465:1243–1250.

39. Li H, Vienna JD, Chen YL, Wang LQ, Liu J. Phase separation in simulated plutonium glasses with phosphate and fluorine and the effect on glass corrosion in water. Scientific Basis for Nuclear Waste Management XX. Materials Research Society 1997;465:277–283.

40. Li H, Vienna JD, Hrma P, Schweiger MJ, Peeler DK. The role of troublesome components in plutonium vitrification. U.S. Department of Energy Plutonium Stabilization and Immobilization Workshop, Washington, DC: U.S. Department of Energy; 1996. p. 241–252.

41. Li H, Vienna JD, Hrma P, Schweiger MJ, Smith DE, Gong M. Borosilicate glasses for immobilization of plutonium-bearing materials. Ceram Trans. 1996;72:399–408.

42. Li H, Vienna JD, Schweiger MJ, Crum JV. Component solubility in lanthanide borosilicate glasses for the vitrification of plutonium oxide and plutonium-bearing materials. Ceram Trans. 1998;87:189–198.

43. Kidari A, Dussossoy JL, Brackx E, Caurant D, Magnin M, Bardez-Giboire I. Lanthanum and neodymium solubility in simplified SiO_2-B_2O_3-Na_2O-Al_2O_3-CaO high level waste glass. J Am Ceram Soc. 2012;95:2537–2544.

44. Schreiber HD, Coolbaugh MT. Solvations of redox ions in glass-forming silicate melts. J Non-Cryst Solids. 1995;181:225–230. Available from: https://doi.org/10.1016/S0022-3093(94)00516-8

45. Darab JG, Li H, Matson DW, Smith PA, MacCrone RK. Chemical and structural elucidation of minor components in simulated hanford low-level waste glasses. In: D'Amico KL, Terminello LJ, Shuh DK.Synchrotron radiation techniques in industry, chemical, and materials science, New York: Plenum; 1996. p. 237–255.

46. Cotton FA, Wilkinson G. Advanced inorganic chemistry. 4th ed. New York: John Wiley & Sons; 1980.

47. Morss LR, Edelstein NM, Fuger J. The chemistry of the actinide and transactinide elements, 3rd ed. Dordrecht, The Netherlands: Springer; 2006.

48. Passerini L. Isomorfismo Tra Ossidi Di Metalli Tetravalenti: I Sistemi: CeO_2 - ThO_2; CeO_2 - ZrO_2; CeO_2 - HfO_2. Gazz Chim Ital. 1930;60:762–776.

49. Caulder DL, Mara MW, Davis LL, Booth CH, Darab JG, Icenhower JP, et al. Hafnium L-edge X-ray absorption near edge structure yields crystal field splitting. 2022. **In Preparation**.

50. Motevalli M, Shah D, Sullivan AC. Solid-state and solution structures of some lithium salts of tetraphenyldisiloxanediolate(2−) and the lithium-bridged compounds $Li_2[M(OSiPh_2OSiPh_2O)_3 \cdot 3Py](Py = Pyridine, M = Zr$ or Hf). Dalton Trans. 1993;(18):2849–2855. https://doi.org/10.1039/DT9930002849

51. Li P, Chen I-W, Penner-Hahn JE, Tien T-Y. X-ray absorption studies of ceria with trivalent dopants. J Am Ceramic Soc. 1991;74(5):958–967. https://doi.org/10.1111/j.1151-2916.1991.tb04328.x

52. Assefa Z, Haire RG, Stump N. Excitation and emission profiles of Cm(III) and Cm(IV) in neat samples and lead borosilicate glasses. Scientific Basis for Nuclear Waste Management XXII, Vol. 556.Warrendale, PA: Materials Research Society; 1999. p. 359–366.

53. Farges F. Structural environment around Th^{4+} in silicate glasses: implications for the geochemistry of incompatible Me^{4+} elements. Geochimica Cosmochimica Acta. 1991;55:3303–3319. https://doi.org/10.1016/0016-7037(91)90490-V

54. Hess NJ, Weber WJ, Conradson SD. X-ray absorption fine structure of aged, Pu-doped glass and ceramic waste forms. J Nucl Mater. 1998;254:175–184.

55. Hess NJ, Weber WJ, Conradson SD. U and Pu L_{III} XAFS of Pu-doped glass and ceramic waste forms. J Alloys Compd. 1998;271–273:240–243.

56. Li LY, Strachan DM, Li H, Davis LL, Qian MX. Crystallization of gadolinium- and lanthanum-containing phases from sodium alumino-borosilicate glasses. J Non-Cryst Solids. 2000;272(1):46–56.

57. Li H, Su Y, Li L, Strachan DM. Raman spectroscopic study of gadolinium(III) in sodium-aluminoborosilicate glasses. J Non-Cryst Solids. 2001;292(1–3):167–176.

58. Vienna JD, Alexander DL, Li H, Schweiger MJ, Peeler DK, Meaker TF. Plutonium dioxide dissolution in glass, PNNL-11346. Richland, WA: Pacific Northwest National Laboratory;1996.

59. Bucher JJ, Allen PG, Edelstein NM, Shuh DK, Madden N, Cork C, et al. A multichannel monolithic Ge detector system for fluorescence X-ray absorption spectroscopy. Reviews in Scientific Instrumentation. 1996;67(9):3361–3365.

60. Antonio MR, Xue JS, Soderholm L. The oxidation state of cerium in Ce_2MoO_6. J Alloys Compd. 1994;207/208:444–448. https://doi.org/10.1016/0925-8388(94)90260-7

61. Bianconi A, Marcelli A, Dexpert H, Karnatak R, Kotani A, Jo T, et al. Specific intermediate-valence state of insulating 4f compounds detected by L_3 X-ray absorption. Phys Rev B. 1987;35:806–812. https://doi.org/10.1103/PhysRevB.35.806

62. Le Normand F, Hilaire L, Kili K, Krill G, Maire G. Oxidation state of cerium in cerium-based catalysts investigated by spectroscopic probes. J Phys Chem C. 1988;92(9):2561–2568. https://doi.org/10.1021/j100320a033

63. Antonio MR, Soderholm L. Cerium valence in cerium-exchanged Preyssler's heteropolyanion through X-ray absorption near-edge structure. Inorg Chem. 1994;33:5988–5993. https://doi.org/10.1021/ic00104a004

64. Brown GE, Calas G, Waychunas GA, Petiau J. X-ray absorption spectroscopy and its applications in mineralogy and geochemistry. In: FC Hawthorne, ed. Spectroscopic methods in Mineralogy and Geology. Chelsea, MI: Mineralogical Society of America;1988.p. 431–512.

65. Schreiber HD. An electrochemical series of redox couples in silicate melts: a review and applications to geochemistry. Journal of Geophysical Research-Atmospheres. 1987;92(B9):9225–9232.

66. Schreiber HD, Balazs GB, Carpenter BE, Kirkley JE, Minnix LM, Jamison PL. An electromotive force series in a borosilicate glass-forming melt. Communication of American Ceramic Society. 1984;67:C106–C108.

67. Veal BW, Mundy JN, Lam DJ. Actinides in silicate glasses. In: AJ Freeman, GH Lander, eds. Handbook on the physics and chemistry of the actinides. New York, NY: Elsevier Science Publisher;1987. p. 271–309.

68. Nugent LJ. Lanthanides and actinides. Inorganic chemistry. Baltimore, MD: University Park Press;1975.

69. Hrma P, Izak P, Vienna JD, Thomas ML, Irwin GM. Partial molar liquidus temperatures of multivalent elements in multicomponent borosilicate glass. Phys Chem Glasses. 2002;43(2):119–127.

70. Hrma P, Vienna JD, Wilson BK, Plaisted TJ, Heald SM. Chromium phase behavior in a multi-component borosilicate glass melt. J Non-Cryst Solids. 2006;352:2114–2122. https://doi.org/10.1016/j.jnoncrysol.2006.02.051

71. Raymond KN, Durbin PW. The design, synthesis and evaluation of sequestering agents specific for plutonium(IV). The First Hanford Separation Science Workshop, Pacific Northwest National Laboratory; 1993, Richland, WA.

SUPPORTING INFORMATION

Additional supporting information can be found online in the Supporting Information section at the end of this article.